Fabrication of x-ray absorption gratings via micro-casting for grating-based phase contrast imaging

2014 J. Micromech. Microeng. 24 015007

(http://iopscience.iop.org/0960-1317/24/1/015007)

IOP Publishing Journal of Micromechanics and Microengineering
J. Micromech. Microeng. **24** (2014) 015007 (5pp) doi:10.1088/0960-1317/24/1/015007

Fabrication of x-ray absorption gratings via micro-casting for grating-based phase contrast imaging

Yaohu Lei, Yang Du, Ji Li, Zhigang Zhao, Xin Liu, Jinchuan Guo and Hanben Niu

Key Laboratory of Optoelectronics Devices and Systems of Ministry of Education, Institute of Optoelectronics, Shenzhen University, Shenzhen 518060, People's Republic of China

E-mail: hbniu@szu.edu.cn

Received 2 September 2013, in final form 19 October 2013
Published 28 November 2013

Abstract

Grating-based x-ray differential phase contrast (DPC) imaging has shown huge potential. For broad applications, it is essential that the key components are low-cost, especially the absorption gratings. We therefore proposed and developed a micro-casting process for fabricating x-ray absorption gratings with bismuth. This process is feasible for mass production at low cost, with a large format, and a high aspect ratio. To develop this kind of absorption grating, an array with deep trenches was fabricated by photo-assisted electrochemical etching in a silicon wafer. The trenches were then filled with bubble-free, molten bismuth via capillary action and surface tension. Bismuth was attractive as a filling material because of its great mass absorption coefficient, low cost and broad environmental compatibility. Furthermore, our micro-casting process provided bismuth absorption gratings with a clean surface and no need for post treatment. To test their performance in x-ray DPC imaging, two bismuth absorption gratings, one as a periodic source and another as the analyzer, were used with periods of 42 and 3 μm and depths of 110 and 150 μm, respectively. The acquired phase-contrast images demonstrated that the micro-casting process produces qualified gratings for x-ray DPC imaging.

Keywords: absorption grating, electrochemical etching, oxidation, phase contrast, bismuth

1. Introduction

During the past decades, x-ray phase contrast imaging has shown to provide a much higher image contrast than conventional x-ray radiography imaging in soft tissues and objects with low-Z elements [1–6]. By replacing the highly brilliant synchrotron source by a low-brilliance conventional x-ray tube and a source grating [7], differential phase contrast (DPC) imaging has attracted more attention than other x-ray phase contrast methods and may find applications in product inspection, medical imaging and other non-destructive observations [8–11].

The source grating generates an array of individually coherent, but mutually incoherent x-ray sources resulting in an efficient use of the available flux. A Talbot interferometer consisting of a phase grating and an analyzer grating is the key component in DPC imaging [12]. Currently, absorption gratings composed by an array of highly absorbing metal lines are usually fabricated by LIGA (lithography, electroplating and molding), which mostly relies on the synchrotron source [13–15]. C David used ingenious fabrication processes with photolithography, anisotropic wet etching and electroplating for absorption gratings in 2007 [8], but their aspect ratio is not sufficient to acquire a high contrast image at high x-ray photon energy. Furthermore, gold is usually chosen as the absorbing metal because of its high absorbing x-ray efficiency [13–15]. However, it requires about 10 g of gold for a large-format analyzer grating. These existing processes and material lead to high cost and limiting the broad dissemination of these components for DPC imaging. Therefore, the mass production of low cost and high aspect ratio absorption gratings through a simple process remains an active area of research.

In this paper, we describe a convenient and economical approach called the micro-casting process to fabricate x-ray absorption gratings in a 5 inch n-type ⟨1 0 0⟩ silicon wafer. The approach involves a three-step process: photo-assisted electrochemical etching in a silicon wafer forming a high aspect-ratio grating structure; surface modification enhancing the infiltration between silicon surface and molten metal; and filling the etched structure with molten metal. The metal bismuth is chosen as the absorbing material because of its great mass absorption coefficient, low cost, environmental compatibility and low toxicity. According to our imaging system design, two x-ray absorption gratings were fabricated with periods of 42 and 3 μm, and depths of 110 and 150 μm, respectively. To verify their microstructure, we used a scanning electron microscope (SEM) and performed an experiment acquiring moiré fringe and a phase-contrast image of a chip in x-ray DPC imaging.

2. Micro-casting for x-ray absorption gratings

Photo-assisted electrochemical etching has been used for the formation of grating structures in n-type ⟨1 0 0⟩ silicon wafer [16–18]. First, a layer of aluminum with thickness of 2 μm is coated on the back side of wafer to provide a uniform electric field distribution through the whole silicon wafer. A 0.3 μm silicon nitride layer is deposited on the front side of wafer. We then use a standard photolithography process to pattern the trenches. Subsequently, a solution of KOH or TMAH with a certain temperature and concentration generates the reverse-pyramid tips [17].

The etching setup consists of five main parts: a Teflon container, power supply, an illumination system, a solution circulation system and a cooling system, similar to previous reports [17, 19]. The fabrication electrolyte is a mixture of deionized water, alcohol and HF. Alcohol removes hydrogen bubble and smooths the surface of the walls [20]. A HF concentration of 5 wt% was used for etching the source grating. Following Lehmann's formula [21], we kept the etching current density corresponding to a specific temperature and solution concentration by adjusting the illumination [17]. A 90 min etching provides a trench array with a depth of 110 μm and wall thickness of 10.5 μm (figure 1(*a*)). A HF concentration of 8 wt% was used for the analyzer grating structure. The concentration at the same etching time leads to a depth of 150 μm, as shown in figure 1(*b*).

There is ample experimental evidence that the physical property between molten bismuth and the silicon surface prevents the filling. A wide enough trench for the source grating appears to easily contain the molten metal and only a little area in the grating surface can be filled. A similar but worse situation happens to the analyzer grating, which has a much smaller period and higher aspect ratio than the source grating. Hence, some procedures, such as the nitridation or oxidation of the silicon surface, known as the surface modification, have to be taken to improve the infiltration.

Compared with nitridation, dry-oxygen oxidation and wet-oxygen oxidation are simple and general methods in the process of surface modification [22]. We choose dry-oxygen oxidation to obtain a more compact SiO_2 layer on the sidewall

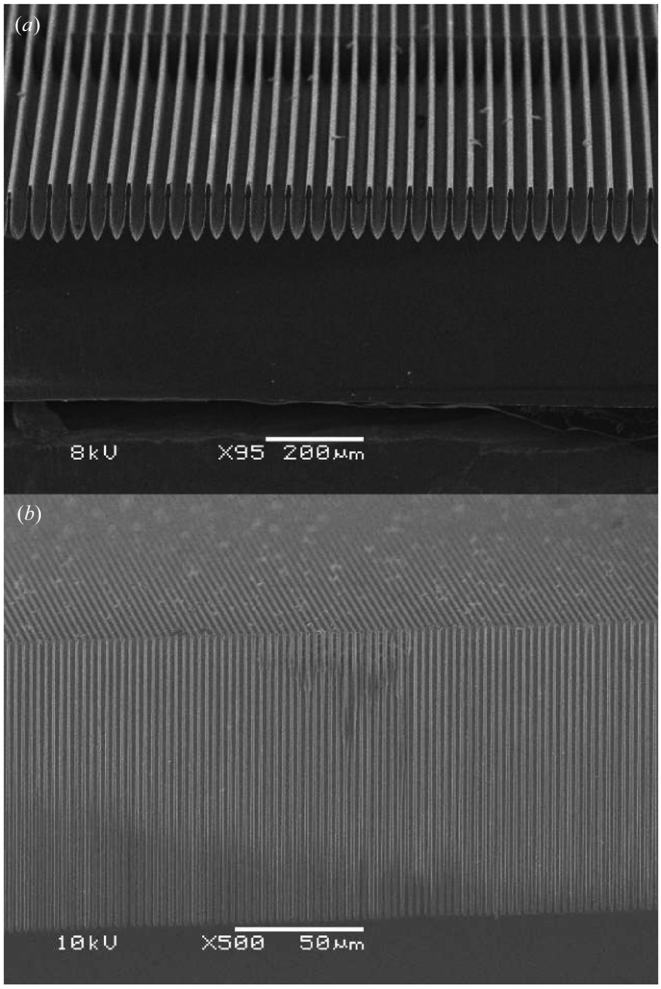

Figure 1. A micrograph of the cross-section of grating structures obtained by SEM. (*a*) The etching image of the structure for the source grating. (*b*) The etching structure for the analyzer grating.

surface. Note that a layer of SiO_2 with at least a thickness of 100 nm should be uniformly achieved to ensure a perfect filling.

A layer of SiO_2, larger than the smallest thickness in the whole blind holes, is covered after the oxidation process at 1100 °C for 1 h. Then the wafer with etching structure is fixed tightly by a stainless steel circular support to adjust the distortion produced during the oxidation. This is fixed on a transmission rod and controlled by the pneumatic device in the high temperature and pressure furnace as shown in figure 2. The main points of this procedure are to exploit the vacuum characteristics of high aspect-ratio trenches for filling with molten bismuth without bubbles and to make the surface of the silicon wafer bismuth-free. When bismuth in the filling container is heated to the melting point, the transmission rod is driven by the pneumatic device to insert the silicon wafer slowly into the filling container. After a short period of time, the molten bismuth is pulled into the trenches by capillary action and surface tension resulting in a uniformity filling. When the silicon wafer is lifted up to the top graphite plate that has the same temperature as the bottom one, we make sure that the molten bismuth in the trenches does not flow out and the residual bismuth on the wafer surface drips down to avoid

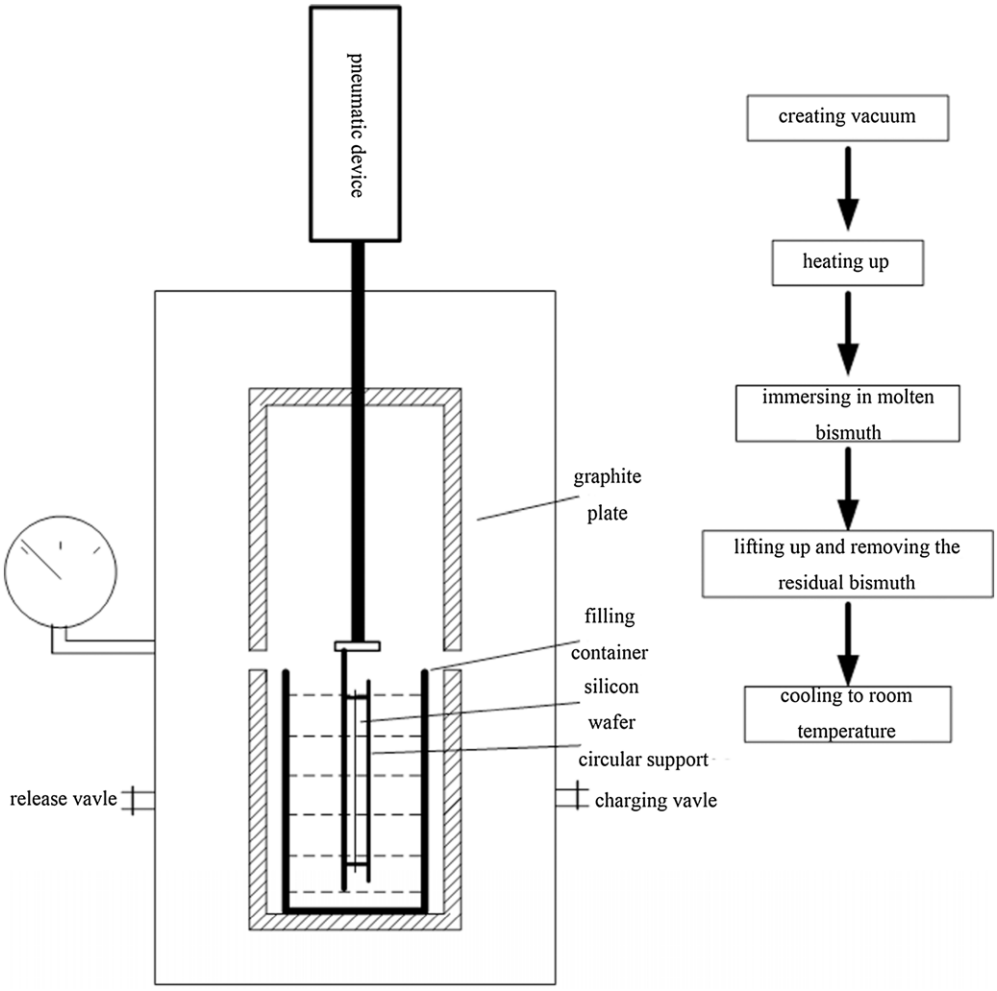

Figure 2. The schematic diagram of high temperature and pressure furnace used for filling metal into the etching structure (left), and the flowchart of filling procedure (right).

a post treatment. Finally, the temperature is slowly decreased to room temperature by a controller.

We choose bismuth as the filling metal for its low-cost advantage and large x-ray absorption coefficient with low toxicity. Gold is the current standard for x-ray absorbing materials because of its high density and mass absorption coefficient. As mentioned above, gold is a noble metal and not suitable for mass production. Other alternatives including lead and bismuth with a density of 11.34 and 9.8 g cm^{-3}, mass absorption coefficient of 27.5 and 28.9 cm^2 g^{-1} at 31 keV can be used as the x-ray absorbing materials. According to the relationship between the incident intensity I_0 and the output intensity I_1 $\frac{I_l}{I_0} = \exp(-\mu_m \rho l)$, we can conclude that the absorption efficiency of gold at 100 μm is the same as lead of 154 μm and bismuth of 170 μm at 31 keV. Here, μ_m is the mass absorption coefficient, ρ, the material density, and l is the x-ray cross-section, respectively [23]. We selected bismuth because of its greater environmental compatibility and lower melting point of 271.3 °C.

3. Test of absorption gratings

The morphology and function of absorption gratings are the two essential aspects of the performance test. Generally,

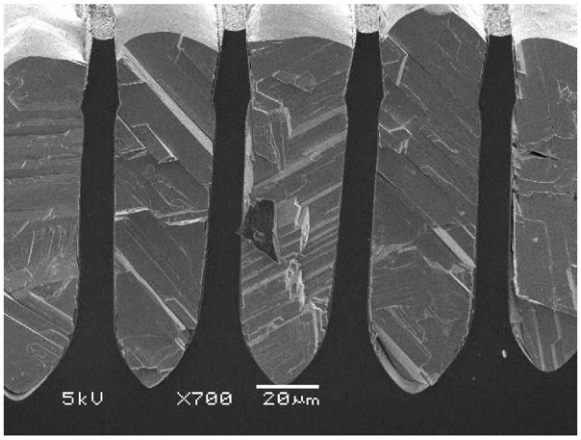

Figure 3. Cross-section view of the source grating imaged by SEM.

microscopy provides good quality, internal-structure images, including the pitch, duty ratio, degree of metal filling and so on. By using absorption gratings in DPC imaging, we can obtain the moiré fringe and the phase-contrast images from which an overall evaluation of these gratings would be acquired.

A micrograph of the cross-section of the source grating is shown in figure 3. The silicon walls and the filled bismuth

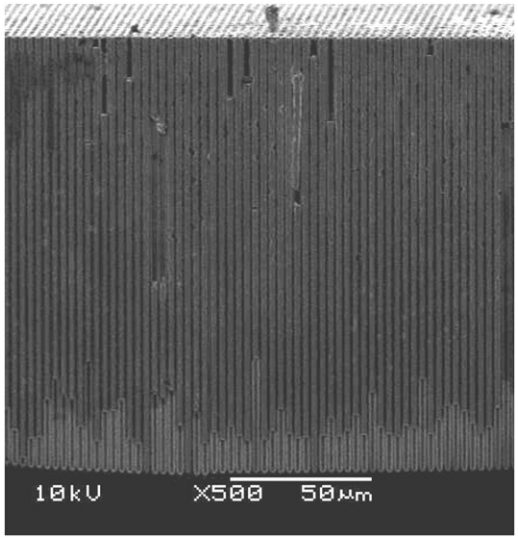

Figure 4. Cross-section view of the analyzer grating imaged by SEM.

part are designed for transmission and absorption of x-rays in order to function as an absorption grating. A duty ratio of 0.25 and 0.5 are used here, respectively. Actually, the silicon wall width is not uniform, but has a gradual change. In addition, wavy filling implies that they are filled more in the middle of a trench than the side position. This is seen in the source grating, but not in the analyzer grating. Fortunately, the minimum and maximum height of the wavy filling are both near to the height of the etching walls. This suggests that the influence on the x-ray contrast at the back of the source grating is small. The wavy filling and wall variation can be observed from the cross-sectional view (figure 3).

The analyzer grating is defined and fabricated as shown in figure 4. In one dimension, it is a periodic structure of silicon walls and filled bismuth. From the top part of the analyzer grating, the trenches are filled with bismuth without any residual bismuth on the surface. Unfortunately, it is not a compact filling from the bottom of trenches. This is attributed to some bubbles remaining in the high aspect-ratio trenches.

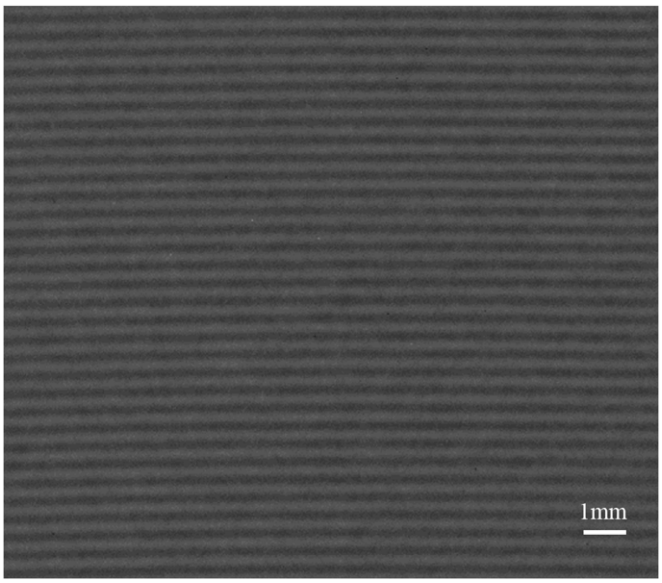

Figure 6. The moiré fringe recorded by the CCD using these absorption gratings in DPC imaging system.

Figure 5 gives a typical DPC imaging system consisting of a source grating G_0, a phase grating G_1, and an analyzer grating G_2 with periods of p_0, p_1 and p_2 and with duty ratios of γ_0, γ_1 and γ_2, respectively. l is the distance between G_0 and G_1, and d is the distance between G_1 and G_2. The parameters in our system are as follows: $p_0 = 42$ μm, $\gamma_0 = 0.25$, $p_1 = 5.6$ μm, $\gamma_1 = 0.5$, and $p_2 = 3$ μm, $\gamma_2 = 0.5$, $l = 1470$ mm and $d = 105$ mm. These are all based on the central wavelength of $\lambda_c = 0.04$ nm, corresponding to conventional tungsten target x-ray source operated at 60 kV. A structured CsI(Tl) scintillator is optically coupled with a cooled CCD camera through a fiber tape with a demagnification of 2 as the imaging detector. We first recorded the moiré fringe by adjusting the angle between the analyzer grating and the phase grating, as shown in figure 6. Finally, making lines of the two gratings parallel, the phase retrieval is completed with a two-step phase stepping from the data recorded by the CCD camera [24, 25]. As shown in figure 7, a phase-contrast image of a chip has been obtained, which is conclusive functional testing of the absorption gratings.

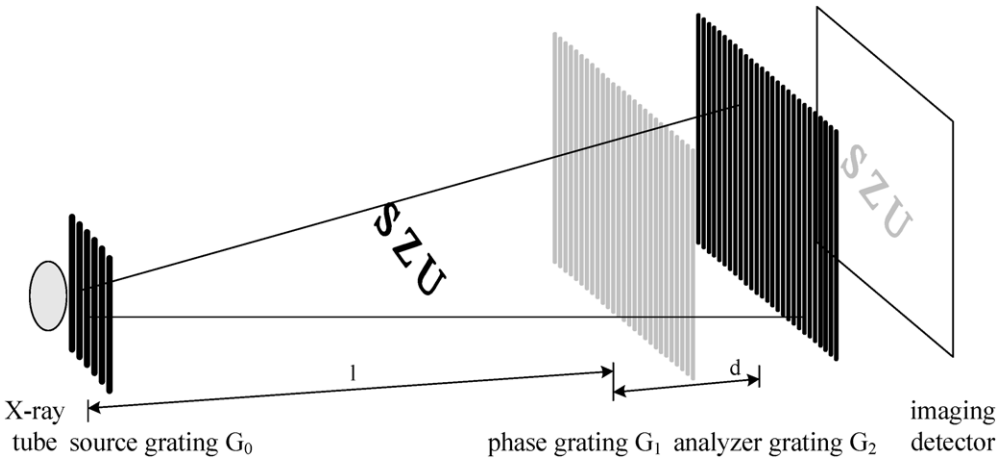

Figure 5. The schematic diagram of the grating-based x-ray phase contrast imaging system.

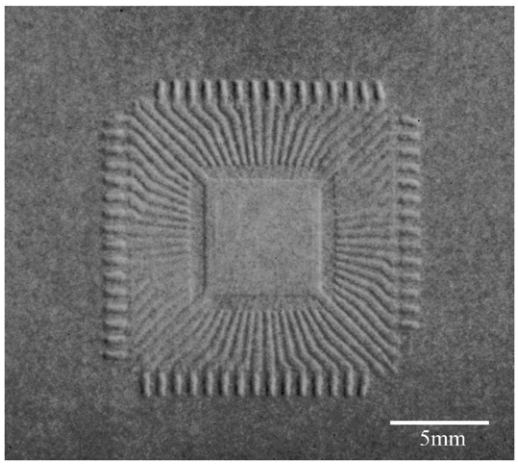

Figure 7. The phase-contrast image of a chip using the imaging system as shown in figure 5.

4. Conclusion

Micro-casting for low-cost x-ray absorption gratings has been developed by a convenient process suitable for mass production. This process involves: photo-assisted electrochemical etching, surface modification and the filling of molten metal bismuth. It has confirmed the qualified characteristics for absorption gratings including the required structures with a high aspect ratio, a large format and a clean surface. Furthermore, the verification of qualified absorption gratings was provided by morphology and functional testing which demonstrated that the micro-casting process is an effective way for fabricating x-ray absorption gratings.

Acknowledgments

This research was supported by the National Special Foundation of China for Major Science Instrument (grants 61227802), and the National Program on Key Basic Research Project (2012CB825802), and the National Natural Science Foundation (NNSF grants 61101175 and 60532090), and the Science & Technology Bureau of Shenzhen (grants JC201005280502A and CXB201005240011A). The authors would also like to thank the Shenzhen Si Semiconductors Co., Ltd. for the high quality silicon wafers, and Mrs Xu for the SEM images.

References

[1] Momose A, Takeda T, Itai Y and Hirano K 1996 Phase-contrast x-ray computed tomography for observing biological soft tissues *Nature Med.* **2** 473–5
[2] Chapman D, Thomlinson W, Johnston R E, Washburn D, Pisano E, Gmur N, Zhong Z, Menk R, Arfelli F and Sayers D 1997 Diffraction enhanced x-ray imaging *Phys. Med. Biol.* **42** 2015–25
[3] Snigirev A, Snigireva I, Kohn V, Kuznetsov S and Schelokov I 1995 On the possibilities of x-ray phase contrast microimaging by coherent high-energy synchrotron radiation *Rev. Sci. Instrum.* **66** 5486–92
[4] Nugent K A, Gureyev T E, Cookson D F, Paganin D and Barnea Z 1996 Quantitative phase imaging using hard x-rays *Phys. Rev. Lett.* **77** 2961–4
[5] Wilkins S W, Gureyev T E, Gao D, Pogany A and Stevenson A W 1996 Phase-contrast imaging using polychromatic hard x-rays *Nature* **384** 335–8
[6] Zanette I, Weitkamp T, Donath T, Rutishauser S and David C 2010 Two-dimensional x-ray grating interferometer *Phys. Rev. Lett.* **105** 248102
[7] Pfeiffer F, Weitkamp T, Bunk O and David C 2006 Phase retrieval and differential phase-contrast imaging with low-brilliance x-ray sources *Nature Phys.* **2** 258–61
[8] David C, Bruder J, Rohbeck T, Grünzweig C, Kottler C, Diaz A, Bunk O and Pfeiffer F 2007 Fabrication of diffraction gratings for hard x-ray phase contrast imaging *Microelectron. Eng.* **84** 1172–7
[9] Bech M, Jensen T H, Feidenhans'l R, Bunk O, David C and Pfeiffer F 2009 Soft-tissue phase-contrast tomography with an x-ray tube source *Phys. Med. Biol.* **54** 2747–53
[10] Momose A, Kuwabara H and Yashiro W 2011 X-ray phase imaging using Lau effect *Appl. Phys. Express* **4** 066603
[11] Du Y, Liu X, Lei Y, Guo J and Niu H 2011 Non-absorption grating approach for x-ray phase contrast imaging *Opt. Express* **19** 22669
[12] Thuering T, Modregger P, Grund T, Kenntner J, David C and Stampanoni M 2011 High resolution, large field of view x-ray differential phase contrast imaging on a compact setup *Appl. Phys. Lett.* **99** 041111
[13] Noda D, Tanaka M, Shimada K, Yashiro W, Momose A and Hattori T 2008 Fabrication of large area diffraction grating using LIGA process *Microsyst. Technol.* **14** 1311–5
[14] Noda D, Tsujii H, Takahashi N and Hattori T 2010 Fabrication of high precision x-ray mask for x-ray grating of x-ray Talbot interferometer *Microsyst. Technol.* **16** 1309–13
[15] Kenntner J *et al* 2010 Front and backside structuring of grating for phase contrast imaging with x-ray tubes *Proc. SPIE* **7804** 780408
[16] Lehmann V and Föll H 1990 Formation mechanism and properties of electrochemically etched trenches in n-type silicon *J. Electrochem. Soc.* **137** 653–9
[17] Lei Y H, Liu X, Guo J C, Zhao Z G and Niu H B 2011 Development of x-ray scintillator functioning also as an analyser grating used in grating-based x-ray differential phase contrast imaging *Chin. Phys.* B **20** 042901
[18] Astrova E V and Fedulova G V 2009 Formation of deep periodic trenches in photo-electrochemical etching of n-type silicon *J. Micromech. Microeng.* **19** 095009
[19] Linnros J, Badel X and Kleimann P 2006 Macro pore and pillar array formation in silicon by electrochemical etching *Phys. Scr.* **T126** 72–6
[20] Lin J C, Lai C M, Jehng W D, Hsueh K L and Lee S L 2008 Effect of ethanol on the photoelectrochemical fabrication of macroporous n-Si(1 0 0) in HF solution *J. Electrochem. Soc.* **155** D436–42
[21] Lehmann V 1993 The physics of macropore formation in low doped n-type silicon *J. Electrochem. Soc.* **140** 2836–43
[22] Zant P V 2004 *Microchip Fabrication: A Practical Guide to Semiconductor Processing* (New York: McGraw-Hill)
[23] Als-Nielsen J and McMorrow D 2011 *Elements of Modern x-ray Physics* (Chichester: Wiley)
[24] Xin L, Jin-Chuan G and Han-Ben N 2010 A new method of detecting interferogram in differential phase-contrast imaging system based on special structured x-ray scintillator screen *Chin. Phys.* B **19** 070701
[25] Liu X, Guo J C, Lei Y H, Du Y and Niu H B 2012 Two-step phase retrieval method with unknown phase shift on non-absorbtion grating x-ray differential phase contrast imaging system *Nucl. Instrum. Methods Phys. Res. A* **691** 86–9